A Calculation of the Effect of Large-Scale Heat Sources on Southern Hemisphere Sub-Tropical Wind Flow

By J. F. DE LISLE and J. F. HARPER[1], New Zealand Meteorological Service, Wellington, N. Z.

(Manuscript received June 7, 1960)

Abstract

The quasi-stationary effects of large-scale heat sources on a baroclinic model atmosphere in which low-level zonal easterly winds decreasing with height are surmounted by zonal westerly winds increasing with height are calculated. Two cases are considered: (1) where the surface of zero zonal wind is parallel to the bottom boundary, (2) where it slopes upwards from this boundary towards the north.

The latter case incorporates roughly the more important features of the mean summer sub-tropical flow in the Australian region.

The results found by calculation were compared with the effects produced in the general circulation in summer by the Australian continent and similarities were found.

1. Introduction

A theoretical treatment of the effect of large-scale heat sources on the baroclinic zonal westerly flow has been given by SMAGORINSKY (1953). He considered the heating as a perturbation on a uniform flow and calculated the steady state field of motion consistent with a given form of heating. His results showed that contrary to the expected result from simple convective considerations, the surface trough was displaced from the position of maximum heating.

When surface friction was taken into account the troughs and ridges sloped upwards towards the west in the lower and middle troposphere and became vertical in the upper troposphere. A comparison of the results with observations on the effects of northern hemisphere heat sources and sinks gave some support for these conclusions.

An independent analysis by GILCHRIST (1954) gave the same type of result and also an explanation of the reversal in the slope of the troughs and ridges between summer and winter as a resonance phenomenon.

In the southern hemisphere the continental heat and cold sources, with the exception of Antarctica, are smaller than those in the northern hemisphere and are in lower latitudes. Also the Andes mountains in South America and the high plateau in South Africa make it certain that in these two continents any effects due to heating would be complicated by those due to orography.

Over Australia where the orographic effects are not as important as in the other two southern continents, the summer heat low is a well known feature of the surface chart. An analysis of 10 years of daily 1100 G.M.T. surface charts for the months November to March has been made by MORIARTY (1955) in which he classified the pressure patterns into 10 types and gave the frequency of occurrence of each type. In 72.5 per cent of the 1513 charts classified, the pressure pattern was some simple modification of that shown in Fig. 1. This shows

[1] Now at Emmanuel College, Cambridge.

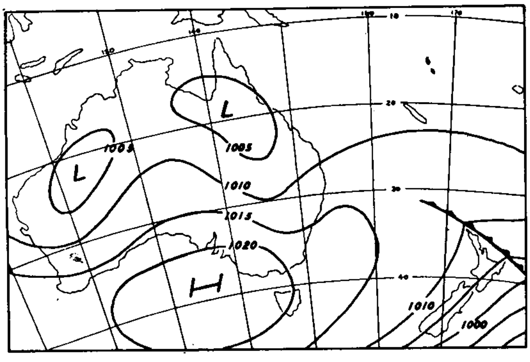

Fig. 1. M.S.L. synoptic chart for 1200 G.M.T. 20 Jan. 1960.

troughs over both eastern and western Australia and a ridge in the centre of the continent. The most commonly occurring pattern was that in which the trough over the west of the continent was more developed than that over the east.

At the 700 mb level on the mean contour chart, the surface heat low over western Australia has been replaced by an anticyclone and there is a trough just off the east coast. This is shown in Fig. 2, the January mean 700 mb chart drawn from "Upper Air Data Australia 1958", compiled by the Commonwealth of Australia, Bureau of Meteorology and from unpublished New Zealand upper air data.

The apparently shallow nature of the heating effect is also shown by the monthly mean upper-level isotherms. January mean isotherms given by PHILLPOT and REID (1953) show a warm pool over NW Australia at both the 850 and 700 mb levels but E—W isotherms at 500 mb.

Thus the observational data available indicate that the large-scale heating effect is confined over Australia to the lower troposphere and that the major surface trough is frequently found over the western part of the continent.

By analogy with the result found by SMAGORINSKY (1953) for heating in a westerly flow in middle latitudes this would seem to show a displacement of the surface trough downstream in the low-level easterlies. However the frequent presence of a second surface trough over the eastern part of Australia makes it certain that no single mechanism can account for the mean summer patterns found.

The present investigation is an attempt to find the effect of large-scale heat sources on a zonal current consisting of low-level easterly winds decreasing with height surmounted by westerly winds increasing with height.

This is the type of mean zonal flow found in the southern hemisphere sub-tropics as shown in the meridional cross section of HUTCHINGS (1950). In this flow the approximately plane boundary of zero zonal wind slopes upwards from the surface towards the north.

A simplified model (Model I) is first considered in which the plane of zero zonal wind is parallel to the lower boundary and the perturbation method is used to find the stationary disturbed flow consistent with a given heating function. The relation of this type of model with that treated by SMAGORINSKY (1953) is shown.

The same type of analysis is then applied to a more realistic model (Model II) with a sloping boundary of zero zonal wind. This model incorporates the most important features of the summer mean flow in the latitudes of Australia but the geometry necessitates a different treatment from that used in Model I.

2. Model I. Horizontal zero zonal wind

Consider a system of rectangular axes with the x axis pointing towards the east, the y axis towards the north and the z axis vertically upwards. Suppose that the steady state zonal flow takes place in a channel

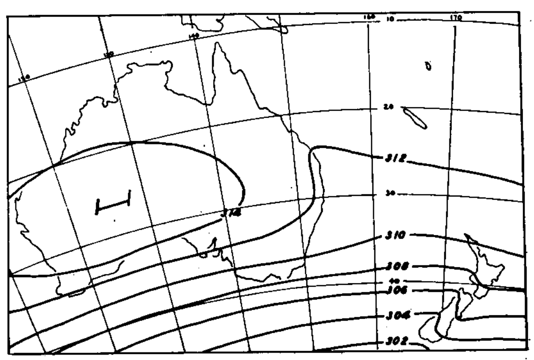

Fig. 2. 700 mb January mean contour chart. Contours in gp dm.

oriented E—W with rigid walls and lid, that the zonal wind U is zero at a height $z = z_0$ and that the vertical wind shear $\Lambda = \frac{dU}{dz}$ is constant with height. Suppose that the plane $U = 0$ is parallel to the bottom boundary so that $U(z) = \Lambda\ (z - z_0)$.

Consider steady state perturbations caused by non-adiabatic heating on the above zonal flow. Assuming geostrophic conditions with incompressible flow, the perturbation vorticity and thermodynamic equations become respectively,

$$U\frac{\partial^2 v}{\partial y^2} + (\beta - U\lambda^2)v = f\left(\frac{\partial w}{\partial z} - \frac{w}{H^*}\right) \quad (1)$$

$$U\frac{\partial v}{\partial z} - \Lambda v + \frac{B^2}{f}w = \frac{gQ}{f} \quad (2)$$

where Q, the perturbation heating function expressed as a rate of heat gained or lost per unit mass and time, is taken to be proportional to exp $i\lambda x$, u, v, w are perturbation velocity components, $\frac{1}{H^*} = \left(\frac{g}{RT_0} - \frac{\gamma}{T}\right)$ where T_0 is the temperature at the surface and γ is the lapse rate, and $B^2 = \frac{g}{T}\left(\frac{g}{c_p} - \gamma\right)$.

The other symbols have their usual meanings.

In (1) the variation of H^* and in (2) of B^2 with height are neglected, T being replaced by $\overline{T}$ the mean temperature of the model.

Elimination of w from (1) and (2) gives

$$U\left(\frac{\partial^2 v}{\partial y^2} + \frac{f^2}{B^2}\frac{\partial^2 v}{\partial z^2}\right) - \frac{Uf^2}{B^2H^*}\frac{\partial v}{\partial z} + $$
$$+ \left(\beta - U\lambda^2 + \frac{f^2\Lambda}{B^2H^*}\right)v = \frac{fg}{B^2}\left(\frac{\partial Q}{\partial z} - \frac{Q}{H^*}\right) \quad (3)$$

Equation (3) which is to be solved in the yz plane has a singularity on the line $U = 0$. However, the singularity may be avoided by the method of cross-substitution (Kuo, 1949) which involves the introduction of internal frictional terms into the equations of motion and a term $\nu \nabla^2\zeta$ into the right hand side of (1) where ν is the kinematic viscosity and ζ the perturbation relative vorticity.

The frictional terms which allow for mixing are very small and become important only in the immediate neighbourhood of $U = 0$.

Now $\nabla^2\zeta$ can be written approximately as

$$\nabla^2\zeta = -\frac{i}{\lambda}\left\{\frac{\partial^4}{\partial y^4} - 2\lambda^2\frac{\partial^2}{\partial y^2} + \lambda^4 + \frac{\partial^4}{\partial y^2\partial z^2} - \lambda^2\frac{\partial^2}{\partial z^2}\right\}v \equiv -iL_1(v)$$

where L_1 is an operator.

Thus with the addition of frictional terms (3) becomes

$$i\nu L_1(v) + UL_2(v) + Mv = \frac{fg}{B^2}\left(\frac{\partial Q}{\partial z} - \frac{Q}{H^*}\right) \quad (4)$$

where L_2 is the operator

$$\left(\frac{\partial^2}{\partial y^2} + \frac{f^2}{B^2}\frac{\partial^2}{\partial z^2} - \frac{f^2}{B^2H^*}\frac{\partial}{\partial z} - \lambda^2\right)$$

and M the multiplier

$$\left(\beta + \frac{f^2\Lambda}{B^2H^*}\right).$$

In the neighbourhood of $U = 0$ we have approximately

$$i\nu L_1(v) + Mv = \frac{fg}{B^2}\left(\frac{\partial Q}{\partial z} - \frac{Q}{H^*}\right) \quad (5)$$

while away from $U = 0$, (3) holds.

Given the form of the heating function Q, it is required to solve (3) and (5) with appropriate boundary conditions. If friction at the lower boundary is introduced in the manner suggested by Charney and Eliassen (1949), w at the surface is given by

$$w = i\left(\frac{-K}{2f}\right)^{\frac{1}{2}}\frac{\sin 2\alpha}{\lambda}\left(\frac{\partial^2 v}{\partial y^2} - \lambda^2 v\right) \quad (6)$$

where K is the eddy diffusivity taken as 10 m^2 sec^{-1} and α is the angle between the isobars and the surface wind taken as 22.5 degrees.

It is assumed that $Q = 0$ on the lateral boundaries and has a maximum at the mid-latitude of the model so that $Q = \chi(z)\sin\mu y$ exp $i\lambda x$ where $\chi(z)$ is the vertical distribution of heating. The solution of (3) and (5) is of the form $v = \{V_1(y,z) + iV_2(y,z)\} \exp i\lambda x$ so that by substituting for v in (3) and separating real and imaginary parts we have away from $U = 0$

$$UL_2(V_1) + MV_1 = \frac{fg}{B^2} \sin \mu y \left(\frac{d\chi}{dz} - \frac{\chi}{H^*}\right) \quad (7)$$

$$UL_2(V_2) + MV_2 = 0 \quad (8)$$

while near $U = 0$

$$M^2V_1 + \nu^2 L_1\{L_1(V_1)\} = \frac{Mfg}{B^2} \sin \mu y \left(\frac{d\chi}{dz} - \frac{\chi}{H^*}\right) \quad (9)$$

$$M^2V_2 + \nu^2 L_1\{L_1(V_2)\} = = -\frac{\nu fg}{B^2} L_1 \left\{\sin \mu y \left(\frac{d\chi}{dz} - \frac{\chi}{H^*}\right)\right\} \quad (10)$$

3. Solution of Equations

As a first approximation to the observed mean summer conditions at lat. 25° S, the mid-latitude of Australia, the following numerical values of constants of the model were taken. $\gamma = 6.5°$ K km^{-1}, $\Lambda = 2$ m sec^{-1} km^{-1}, $f = -0.6 \times 10^{-4}$ sec^{-1}, $\overline{T} = 260°$ K which makes $H^* = 9.4$ km and $B^2 = 1.32 \times 10^{-4}$ sec^2. The lateral boundaries of the model were put for convenience at 38.05° S ($y = 0$) and 11.95° S ($y = 2.899 \times 10^6$ m) and a rigid upper boundary at $z = 12$ km. z_0 was taken as 6 km.

In the almost complete absence of observational data on large-scale heat sources in the southern hemisphere, it was assumed that in the latitudinal belt considered, non-adiabatic heating decreased exponentially with height and could be written $Q = N \sin \mu y \exp \left(i\lambda x - \frac{z}{h}\right)$ where h, N are constants with dimensions km and sec^{-1} respectively. N depends on the values taken for h and the maximum value of the heat perturbation.

In a global study by BLACK (1955) monthly charts are given showing the total solar radiation from sun and sky received at the earth's surface. The charts for the summer months December, January and February show maxima of 650—750 cal cm^{-2} day^{-1} in latitudes 25°—35° S over the continents. If we consider differences from zonal means as perturbation values, this gives over the continents at latitude 25° S a perturbation in total radiation of approximately 250 cal cm^{-2} day^{-1}.

Over central Australia the summer rainfall is small so that most of the non-adiabatic heating is by vertical eddy conduction of sensible heat. In northern Australia however monsoon rains add to the atmosphere heat of condensation of the order of 350 cal cm^{-2} day^{-1}. The latitudinal average rainfall over the oceans at 15° S is given by RIEHL (1954) as 25 cm per summer season, so that the perturbation latent heat added to the atmosphere over northern Australia is approximately 150—200 cal cm^{-2} day^{-1}.

The use of a sine function instead of a step function to describe the variation of heating in the E—W direction over Australia is given some support from the January mean cloudiness figures. In latitudes 25—30° S these tend to show a minimum in the centre of the continent. The variation of heating in the N—S direction is not so well described and in the neglect of the latent heat added at the northern boundary does not correspond with reality.

The maximum heating was taken as 250 cal cm^{-2} day^{-1}, and for $h = 1$ km, N evaluated. The wavelength in the E—W direction was taken as 120 degrees of longitude to simulate roughly the effects of the three southern continents.

If in (9) and (10) ν is taken as 10^{-5} m^2 sec^{-1} and the above values substituted for the other constants, it is found that the effect of the multiplier M^2 swamps that of the operator $\nu^2 L_1\{L_1\}$ so we have to a good approximation

$$MV_1 = \frac{fg}{B^2} \sin \mu y \left(\frac{d\chi}{dz} - \frac{\chi}{H^*}\right) \quad (11)$$

$$V_2 = 0 \quad (12)$$

The lower boundary condition is found by substituting for w from (6) in (2). Separating real and imaginary parts this gives

$$c^2 \nabla_H^4 V_1 + U^2 \frac{\partial^2 V_1}{\partial z^2} - U\Lambda \frac{\partial V_1}{\partial z} + \Lambda^2 V_1 = = \left(U\frac{\partial}{\partial z} - \Lambda\right) \frac{g\chi}{f} \sin \mu y \quad (13)$$

$$c^2 \nabla_H^4 V_2 + U^2 \frac{\partial^2 V_2}{\partial z^2} - U\Lambda \frac{\partial V_2}{\partial z} + \Lambda^2 V_2 = \\ = c\left(\frac{\partial^2}{\partial y^2} - \lambda^2\right) \frac{g\chi}{f} \sin \mu y \qquad (14)$$

where

$$c = B^2 \frac{\sin 2\alpha}{f^2 \lambda} \left(\frac{-Kf}{2}\right)^{\frac{1}{2}} \text{ and } \nabla_H^4 = \\ = \frac{\partial^4}{\partial y^4} - 2\lambda^2 \frac{\partial^2}{\partial y^2} + \lambda^4$$

At $y = 0$ and $y = \frac{\pi}{\mu}$ we have $V_1 = V_2 = 0$.

At the upper rigid boundary we have from (2)

$$U \frac{\partial V_1}{\partial z} - \Lambda V_1 = g\chi \sin \mu y \qquad (15)$$

$$V_2 = 0 \qquad (16)$$

The equations to be solved for V_1, V_2 are (7) and (8) and the boundary conditions are (13)—(16). Also (11) and (12) must be satisfied in the interior of the region at $z = z_0$.

By separation of variables in (8) it is found that the solution is of the form $V_2 = Z_2(z) \sin \mu y$. By making the transformation $z' = (z - z_0)$, $Z_2 = \xi_2 (z') \exp c'z'$ in (8) it is found that if $c' = \frac{1}{H^*} \pm \varepsilon$ where $\varepsilon^2 = \frac{1}{H^{*2}} + 4 \frac{(\lambda^2 + \mu^2)}{f^2} B^2$ and if $z'' = \varepsilon z'$, (8) transforms to the confluent hypergeometric equation

$$z'' \frac{d^2 \xi_2}{dz''^2} - z'' \frac{d\xi_2}{dz''} + \frac{MB^2}{f^2 \Lambda \varepsilon} \xi_2 = 0 \qquad (17)$$

With the values of the constants given above, $\frac{MB^2}{f^2 \Lambda \varepsilon} = 1$ so that the solutions of (17) are $\xi_2 = z''$ and

$$\xi_2 = z'' \left\{ \ln z'' + \sum_1^\infty \frac{z''^n}{(n+1)!n} \right\} - 1 \equiv \psi_1(z'')$$

Thus

$$V_2 = \exp c'(z - z_0) \sin \mu y \\ \{c_1 \varepsilon (z - z_0) + c_2 \psi_1(\varepsilon(z - z_0))\}$$

where c_1 and c_2 are arbitrary constants.

As $\frac{dV_2}{dz}$ must remain finite at $U = 0$, $c_2 = 0$ and because of (12) and (16) we have

$$V_2 = 0 \text{ above } U = 0 \qquad (18)$$

$$V_2 = c_1 \varepsilon (z - z_0) \exp c'(z - z_0) \sin \mu y \qquad (19) \\ \text{below } U = 0$$

By applying similar transformations as above to (7) we find

$$z'' \frac{d^2 \xi_1}{dz''^2} - z'' \frac{d\xi_1}{dz''} + \xi_1 = V_3 \exp az'' \qquad (20)$$

where

$$V_3 = -\frac{gN}{f\Lambda\varepsilon} \left(\frac{1}{h} + \frac{1}{H^*}\right) \exp - \frac{z_0}{h}$$

and

$$a = -\left(c' + \frac{1}{h}\right) \frac{1}{\varepsilon}$$

One solution of (20) is

$$\psi_2(z'') = V_3 \left\{ 1 + \sum_{r=2}^\infty \frac{a + a^2 + \ldots + a^{r-1}}{r!(r-1)} z''^r \right\} \qquad (21)$$

and the complete solution is

$$V_1 = \exp c'(z - z_0) \cdot \sin \mu y \\ \{\psi_2(\varepsilon(z - z_0)) + c_3 \varepsilon (z - z_0) + c_4 \psi_1(\varepsilon(z - z_0))\} \qquad (22)$$

where c_3 and c_4 are arbitrary constants and as before $c_4 = 0$.

From (11) and (12) we have to a good approximation explicit values for v on $U = 0$. This gives an extra boundary condition and implies that the solution in the top and bottom halves of the model can be carried out independently.

Because of the introduction of internal frictional terms in the vicinity of $U = 0$, the simple thermal wind equation will no longer hold there. Therefore if we assume that v and the temperature perturbation are continuous across $U = 0$, $\frac{\partial v}{\partial z}$ need not be continuous. In (22), c_3 for the layer below $U = 0$ will be found from the bottom boundary condition and c_3 for the upper layer from the upper boundary condition.

4. Numerical results from Model I

Equations (17) and (20) were solved with appropriate boundary conditions for the case of $z_0 = 6$ km. The results showing the perturbation meridional velocities for an E—W section through the latitude of maximum heating are shown in Fig. 3.

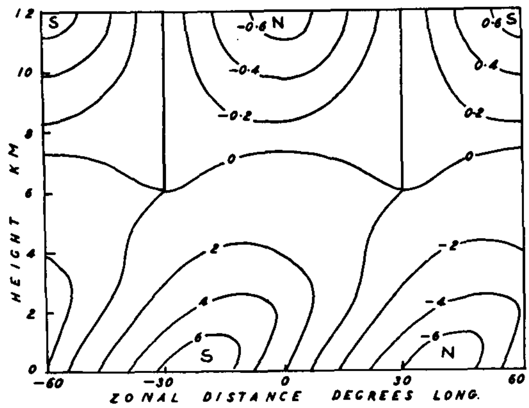

Fig. 3. Perturbation meridional velocities v in m sec^{-1} calculated for E—W section through latitude of maximum heating in Model 1. Zero longitude taken as position of maximum heating.

From this result it is seen that, (a) the velocities above $U = 0$ are an order of magnitude smaller than those below, (b) the troughs and ridges slope upwards towards the east in the lower layers, (c) above $U = 0$ the patterns have no phase change with height and are arranged in a cellular form bounded by lines of zero v.

The surface trough was 6.8 degrees of longitude E of the position of maximum heating.

Both Gilchrist and Smagorinsky found that the slope of the troughs and ridges and their position relative to the heat sources and sinks was dependent on λ, μ and the steady state zonal wind profile. In the frictionless case we have a resonance phenomenon with a phase change in passing through the resonant frequency. In the model with friction at the ground there occur resonant frequencies at which the amplitude of the perturbations is a finite maximum but a phase change still occurs.

In Model I, the zonal wind profile for constant Λ is a function of z_0, the height of $U = 0$, and the value of z_0 to give resonance in the non-frictional case can be found by substituting for V_1 from (22) into (13) and letting $c \to 0$. The coefficient of $c_3 = \sin \mu y \cdot \varepsilon \Lambda^2 z_0^2 c' (1 - z_0 c')$ and solving for z_0 resonance is given by $z_0 = 0, 0, \frac{1}{c'}$.

Thus there is a phase change when z_0 changes from positive to negative values and another on passing through $\frac{1}{c'}$. A negative z_0 changes the basic flow into westerlies at the surface increasing with height and gives the case dealt with by Smagorinsky.

5. Model II. Sloping surface $U = 0$

A model in which the unperturbed flow approximates more closely to the mean summer zonal flow between latitudes 15°—35° S than that so far considered, is given by taking a surface of zero zonal wind sloping upwards from ground level at latitude 35° S towards the north. The flow again is assumed to take place in a latitudinal belt oriented E—W with rigid walls and lid.

If in the N—S section through the model, the line $U = 0$ slopes diagonally and if Λ is constant with height, $U = U(y, z)$ being given by

$$U(y, z) = \Lambda(z - \eta y) \tag{23}$$

where η is the slope of $U = 0$, assumed constant.

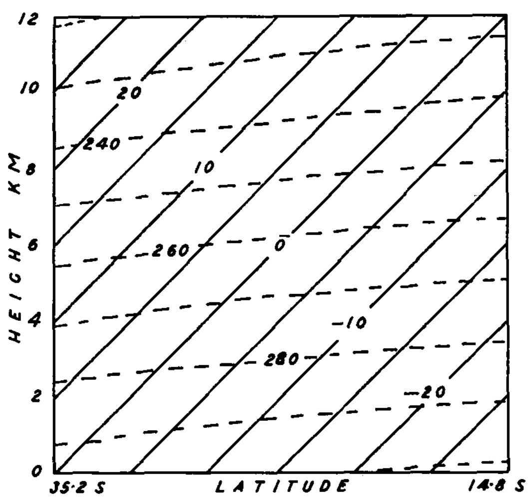

Fig. 4. Steady state zonal wind field U in m sec^{-1} (full lines) and zonal temperature field T in degrees K (dashed lines) for Model II.

If as an approximation to the observed mean summer conditions over Australia we take $\eta = 5.3 \times 10^{-3}$ and for convenience alter the latitudinal width of the model slightly to $y = 2.258 \times 10^6$ m, keeping the other constants of the model the same, the steady state wind field is as shown in Fig. 4.

Assuming the distribution of U given by (23) and that $\frac{\partial T}{\partial z} = -\gamma =$ constant, the steady state temperature field may be found by solving the thermal wind equation as a Lagrangian linear equation. This gives

$$T(y, z) = \left(T_0 + \frac{\gamma \eta g}{fA}\right) \exp\left(\frac{-fAy}{g}\right) - \\ - \gamma\left(z - \eta y + \frac{\eta g}{fA}\right)$$

where T_0 is the temperature at $y = z = 0$, the line where $U = 0$ cuts the lower boundary. Taking $T_0 = 295°$ K the steady state field is shown in Fig. 4.

A comparison of the U and T fields with the mean summer cross section given by HUTCHINGS (1959) shows that although the model exaggerates the strength of the tropical easterlies, it incorporates roughly the general features of the mean tropospheric flow in the latitudinal belt of the Australian continent.

If a similar system of heat sources to that in Model I is applied to the above steady state, the equation to be solved for v is (3) where U is given by (23). Since $U = U(y, z)$ the variables cannot be separated and (3) had to be solved by numerical methods.

As before (7) and (8) were solved for V_1 and V_2 respectively, while the boundary conditions were,

(a) $V_1 = V_2 = 0$ on the lateral boundaries
(b) Eq. (11) and (12) on the line $U = 0$
(c) Eq. (13) and (14) on the lower boundary
(d) Eq. (2) with $w = 0$ on the upper boundary
(e) $\zeta = 0$ and therefore $\frac{\partial^2 v}{\partial y^2} = 0$ at $z = 0$ on the lateral boundaries.

Relaxation methods of solution were used. The relaxation was carried out separately for V_1 and V_2 in the yz plane at the longitude of maximum heating taken as $x = 0$. The rather arbitrary boundary condition (e) above was required because the finite difference approximation to the lower boundary condition requires one fictitious grid point outside the walls.

Before relaxation, the axes were first transformed by writing $y_1 = \frac{y}{10^2 H^*}$ and $z_1 = -\frac{B}{f}\frac{z}{10^2 H^*}$. With the values of the constants given above, the yz cross section of the model transforms to a square of side 2.4 units and the line $U = 0$ becomes a diagonal of the square.

The grid length of the relaxation net was taken as $\Delta y_1 = \Delta z_1 = 0.4$ corresponding to $\Delta y = 377$ km and $\Delta z = 2$ km. Thus 49 grid points were taken and because of the boundary conditions on $U = 0$ the relaxation could be carried out in two independent halves.

The results of the relaxation for the case $h = 1$ km are given in Fig. 5 which shows v in m sec^{-1} for a N—S section through the longitude of maximum heating. Fig. 6 computed from the values used in Fig. 5 shows v for an E—W section through the mid-latitude of the model corresponding to lat. 25° S.

The trough at the surface is 13.4 degrees of longitude downstream from the position of maximum heating and slopes towards the E in the lower troposphere becoming almost vertical at about 6 km. Here it is approximately a quarter of a wavelength E of $x = 0$.

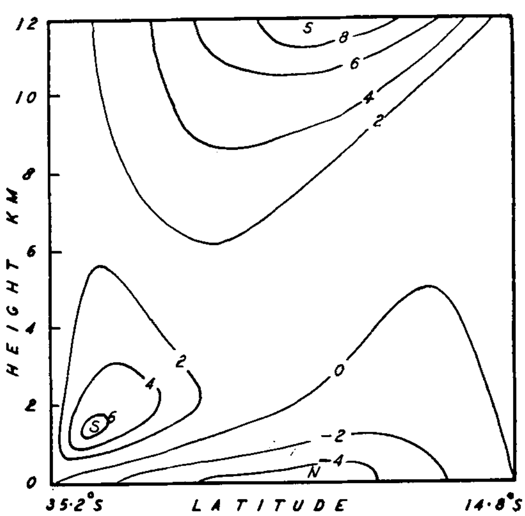

Fig. 5. Perturbation meridional velocities v in m sec^{-1} calculated for a N—S section through longitude of maximum heating in Model II.

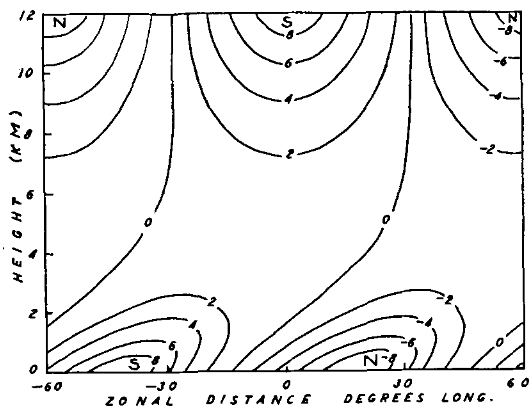

Fig. 6. Perturbation meridional velocities v in m sec^{-1} calculated for an E—W section through latitude of maximum heating in Model II. Zero longitude taken as position of maximum heating.

The w field given in Fig. 7 for an E—W section through the mid-latitude shows maxima in the lowest layers and negligible velocities above 5 km. In the region of the trough, above the horizontal convergence at the surface, there is horizontal divergence up to about 2 km, above which there is weak horizontal convergence.

The results for $h = 2$ and 3 km, which are not shown, gave broadly similar patterns to those for $h = 1$ km. In the case of $h = 2$ km, v is smaller in the lower levels than the values given in Fig. 5 and the surface trough is only 0.3 degrees of longitude downstream from $x = 0$.

In the upper levels where the heating is greater than in the case of $h = 1$ km, large and unrealistic values of v were found. These are partly due to the effect of the upper rigid boundary. However, because of the approximate boundary conditions given by (11) and (12) they have no effect on the perturbations in the easterly flow.

When $h = 3$ km, the surface trough is 3.9 degrees of longitude upstream from $x = 0$.

6. Discussion of Results

Because of the incomplete correspondence between the model and observed sub-tropical flow and the absence of observational evidence on the large-scale heating process it is impossible to get more than a qualitative result by this type of analysis.

Especially at the northern boundary the correspondence with observation is faulty due to
(a) the increasing error towards the north of the geostrophic approximation,
(b) the unperturbed E winds being too large,
(c) non-adiabatic heating not tending to zero in the north of Australia.

The artificial rigid walls in the model also have considerable effect on the flow in the regions where $U = 0$ meets the upper and lower boundary surfaces.

In the N—S section of the model through the longitude of maximum heating, v is zero at the origin and on the side walls and has from (11) a maximum between the origin and the first grid point on $U = 0$. According to the numerical values taken in the heating function large horizontal and vertical shears of v could occur while the scale of motion is small being restricted by the boundaries. It is unlikely that in this region the flow will be geostrophically controlled.

However, at the mid-latitude of the model, the effects due to the boundary conditions are a minimum and with a suitable choice of parameters a realistic result is found there.

Because no analytical solution was found for Model II and the computations were done by hand relaxation it was not possible to find the conditions necessary for resonance. However a comparison of Figs. 6 and 3 shows the effect on the solutions of making the boundary $U = 0$ a sloping surface.

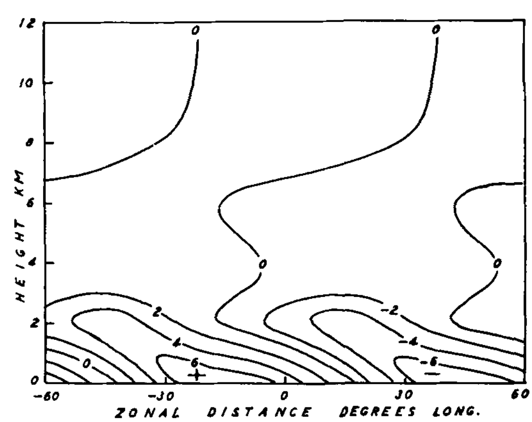

Fig. 7. Perturbation vertical velocities w in 10^{-1} cm sec^{-1} calculated for E—W section through latitude of maximum heating in Model II. Zero longitude taken as position of maximum heating.

In both models the patterns in the lower 6 km are similar. The troughs and ridges in mid-levels are E of those at the surface. The surface troughs and ridges, though, have different positions relative to the position of maximum heating in the two models.

Heating produces quite different results above $U = 0$ in the two models. On the sloping boundary in Model II, the boundary conditions (11) make v near $U = 0$ large with a maximum of $v = 6$ m $\sec^{-1}$ at a height of 1 km. This combined with the effect of the rigid upper boundary gives values of v an order of magnitude greater than those found in Model I where the perturbation on $U = 0$ is small ($v = 0.2$ m $\sec^{-1}$).

In both models there is no phase change with height above $U = 0$ but the cellular pattern evident in Model I with its line of zero v almost parallel to the surface is no longer present. There has been a phase change of 180 degrees in the E—W direction giving the more realistic pattern shown in Fig. 6.

The displacement of the major surface trough in Fig. 1 from the position of maximum heating taken as the centre of the continent is approximately equal to that given by Model II in the case of $h = 1$ km. Also the 700 mb trough ov :r the east coast of Australia in the January mean chart (Fig. 2) is consistent with the upper trough in the model.

In his frequency analysis of surface patterns, MORIARTY (1955) found that the surface pressure system in which there was a single heat low over Eastern Australia did not occur while that in which there was a single low over Central Australia occurred on only 4.3 per cent of the occasions studied. The solutions produced by Model II when $h \geqslant 2$ km thus rarely correspond with the surface heat low patterns found by observation.

The weaker surface trough over E Australia (known as the Cloncurry Low) frequently found in conjunction with the major trough to the west cannot be explained as a heating process of the type suggested here. Since the Cloncurry Low can occur in winter as well as summer, it is probably formed orographically by the action of the mountains along the east coast on the low-level easterly winds.

The results produced by Model I for any positive values of z_0, the height of $U = 0$,

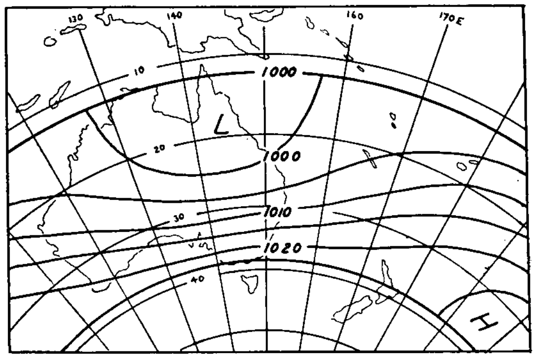

Fig. 8. Surface pressure chart computed for perturbed flow in Model I. Longitude of maximum heating taken as 135° E and E—W wavelength of heating function 120° longitude.

gave a surface pattern with a well developed Cloncurry Low. This is shown in Fig. 8 which has been computed geostrophically taking the pressure at the northern boundary arbitrarily as 1000 mb. The greatly exaggerated E winds to the north of the anticyclone and to the south of the low are caused by the rigid walls.

In order to produce a surface pattern with a trough over W. Australia for the same values of λ, μ and Q as taken in Model I, the surface $U = 0$ must be sloping.

The surface chart calculated from Model II for the same heating function as used in Fig. 8 is shown in Fig. 9.

It is noticed that the trough although centred over W. Australia is not nearly as well developed as that in Model I and that there are similar large velocities caused by the rigid

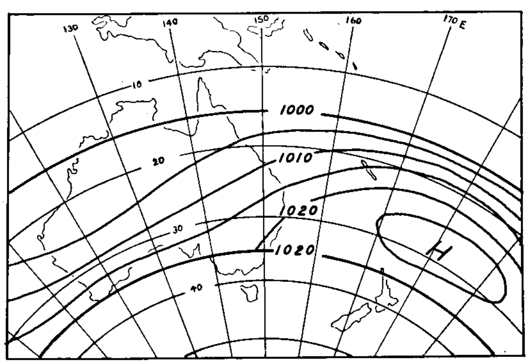

Fig. 9. Surface pressure chart computed for perturbed flow in Model II. Longitude of maximum heating and E—W wavelength of heating function as in Fig. 8.

boundaries. The pattern would look considerably more realistic if the steady state anticyclonic vorticity were reduced by reducing either Λ the vertical shear or η the slope of the surface $U = 0$.

Thus the type of mechanism considered in Model II can account for the major heat low in Australia which is found by observation frequently to be confined to the lower troposphere over the western part of the Continent. The treatment given in Model I can give some information about conditions near the $U = 0$ surface because analytical solutions are possible but cannot produce realistic solutions.

REFERENCES

BLACK, J. N., 1955: The distribution of solar radiation over the earth's surface. *Archiv für Met., Geoph. und Bioklim.*, Ser. B, **7**, pp. 165—189.

CHARNEY, J. G., 1947: The dynamics of long waves in a baroclinic westerly current. *J. Meteor.*, **4**, pp. 141—162.

CHARNEY, J. G. and ELIASSEN, A., 1949: A numerical method for predicting perturbations. *Tellus*, **1**, pp. 38—54.

GILCHRIST, B., 1954: Seasonal changes of thermal perturbations. *Proc. Toronto Met. Conf.* 1953. pp. 129—131.

HUTCHINGS, J. W., 1950: A meridional cross section for an oceanic region. *J. Meteor.* **7**, pp. 94—100.

KUO, H., 1949: Dynamic instability of two-dimensional nondivergent flow in a barotropic atmosphere. *J. Meteor.* **6**, pp. 105—122.

MORIARTY, W. W., 1955: Heating effects over Australia. *Tech. Paper No* **7**. Div. Met. Phys. C.S.I.R.O. Australia. 31 pp.

PHILLPOT, H. R. and REID, D. G., 1953: Upper air temperatures for the Australian region. *Bull. No 42*, Comm. Met. Bur. Australia. 47 pp.

RIEHL, H., 1954: *Tropical Meteorology*. McGraw-Hill Pub. Co. New York. 392 pp.

SMAGORINSKY, J., 1953: The dynamical influence of large-scale heat sources and sinks. *Quart. J. R. Met. Soc.* **79** pp. 342—366.